Comparisons of various model fits to the Iron line profile in MCG-6-30-15

R. Misra

Inter-University Centre for Astronomy and Astrophysics, Pune, India

F. K. Sutaria

Inter-University Centre for Astronomy and Astrophysics, Pune, India

Received ______________; accepted ______________

ABSTRACT

The broad Iron line in MCG-6-30-15 is fit to the Comptonization model where the line broadening occurs due to Compton down- scattering in a highly ionized optically thick cloud. The results are compared to the disk line model where the broadening is due to Gravitational/Doppler effects in the vicinity of a black hole. We find that both the models fit the data well and it is not possible to differentiate between them by fitting the ASCA data only. The best fit temperature and optical depth of the cloud was found to be $kT = 0.54$ keV and $\tau = 4.0$ from the Comptonization model. This model further suggests that while the temperature can be assumed to be constant, the optical depth varied during the observation period. We point out that simultaneous broad band data $(3 - 50$ keV) can rule out (or confirm) the Comptonization model.

We show that the data can also be fit by a narrow line if the underlying continuum is a broken power-law with break energy $E_b \approx 6$ keV, however the high energy photon spectral index turns out to be 2.5 which seems to be in conflict with the earlier Ginga data.

Subject headings: accretion disks—black hole physics—galaxies:individual (MCG-6-30-15)—galaxies:Seyfert—line:profile

1. Introduction

A long ($\approx$ 4.5 days) observation by ASCA of the Seyfert 1 MCG-6-30-15 revealed that the Iron line profile in this source is broad (Tanaka et al. 1995). A more detailed analysis of the data by Iwasawa et al. (1996) showed that the profile is variable and the line width is maximum when the source intensity is minimum. Broad Iron lines have also been detected in other AGN by ASCA (e.g. Nandra et al. 1997). The most straight forward interpretation of this feature is the disk line model where the line is broadened due to the combined effects of Doppler and gravitational red-shift in the vicinity of a black hole (Fabian et al. 1989). Iwasawa et al. (1996) showed that the disk producing this line has to have an inner radius $\approx 1.2 r_s$ where $r_s = GM/c^2$ is the Schwarzschild radius. This would imply that the black hole is spinning close to its maximal value. If this interpretation is correct then this would be the first direct observation of the strong gravitational effects expected in the vicinity of a black hole. Theoretical models will be strongly constrained. The inner disk region has to be cold in order to produce the Iron line while at the same time the hard X-ray producing region would also have to be located close to the inner edge of the disk. Reynolds & Begelman (1997) have argued that if some of the Iron line emission arises from the region inside the last stable orbit, the black hole need not be a rotating one.

Sulentic et al. (1998) showed there was disagreement between the inclination angle derived by fitting the Iron line profile and those from HI and Hα measurements. Several AGN for which a broad Iron line was detected have the peak centroid close to 6.4 keV (Nandra et al. 1997). Sulentic, Marziani & Calvani (1998) point out that this is not expected if the disks are oriented in random directions. They propose that the Iron line profile is a sum of two independent Gaussian lines in order to explain the different correlation relationships of the red and blue side with the source intensity. They also claim that there is a blue wing in the Iron line emission which cannot be explained by the disk line model. These discrepancies and the importance of the implication of the disk line model warrant a study of alternate models to explain the phenomenon.

An alternate model to the disk line one is that the line is intrinsically narrow and it get broadened due to Compton down scattering of the photons as they pass through an optically thick cloud. This model referred to here as the Comptonization model was proposed by Czerny, Zbyszewska and Raine (1991). Fabian et al. (1995) argued that the surrounding Comptonizing cloud has to have a radius $R < 10^{14}$ cms in order that the cloud is highly ionized and does not produce strong absorption lines. For a $10^7 M_\odot$ black hole this would imply that the Iron line producing region is smaller than $50 r_s$ and gravitational effects would be important. The lack of a blue wing in the best fit line profile implied that the temperature of the cloud should be $kT < 0.2$ keV. This is in apparent conflict with the expected Compton temperature of the cloud. Further a break in the continuum around 20 keV is expected for this model which has not been observed. Misra & Kembhavi (1998) point out that for a smaller sized black hole, the intrinsic Iron line produced may not be significantly broadened by gravitational effects. They calculated the equilibrium temperature of the cloud to be around 0.2 keV provided a large UV bump is assumed to be present in this source. They further showed that the earlier $2 - 18$ keV range data from Ginga obtained from this source is not in conflict with this model. The Comptonizing model raises several questions regarding the stability, geometry and dynamics of such a cloud. The origin of such cloud(s) is unspecified but some arguments for their existence are presented by Guilbert & Rees (1988) and Kuncic, Blackman & Rees (1996). Optically thick obscuring clouds may be responsible for the intensity dip in MCG-6-30-15 (McKernan & Yaqoob 1998). In this paper, we fit the Comptonization model to the Iron line profile and compare the results with fits to the disk line model. We constrain the parameters of the Comptonization model and discuss the implications of their values.

The broad line may also be an artifact of simplistic modeling of the continuum. If the underlying continuum is complex and not a simple power-law, residuals caused by this fit may have been interpreted as a broad line. In order to test this hypothesis, we fit the data to a narrow line and a broken power-law as the continuum.

In the next section we briefly describe the observations and data analysis technique, In §3 the three models used for the fitting are described. In §4 the results of the data analysis is presented. In §6 we discuss the implications of the results and summarize the paper in §7.

2. Observations

ASCA observed MCG-6-30-15 from 1994 July 23 to 27 (Tanaka, Inoue & Holt 1994) and the data has been analyzed in detail by Iwasawa et al. (1996). In this paper, we analyze the $3 - 10$ keV data since below 3 keV the spectrum is affected by the partially ionized gas ("the warm absorber") surrounding the source. Following Iwasawa et al. (1996), the data set was divided into three epochs of which the epoch labeled "high" encompasses the highest intensity level of the source. The epoch labeled "low" encompasses the lowest intensity level of the source. The rest of the observation was grouped into a single data set labeled "medium". Data from all four SIS chips were grouped and analyzed. The relative normalization between these four chips was allowed to vary, but in all cases the variation was found to be less than 2%.

3. Models

3.1. Disk Line model

The disk line model of Laor (1991) assumes that the emission arises from an accretion disk around a black hole and includes general relativistic effects. The inner radius of the accretion disk is r_i, where $r_i = 1.235r_s$ and $r_i = 6r_s$ ($r_s = GM/c^2$) correspond to the case of a maximally rotating black hole and a non-rotating one respectively. The model is parameterized by r_i, the outer radius r_o, the emissivity index ξ, the rest frame line energy (fixed at 6.4 keV) and line intensity. The emissivity index (ξ) specifies the dependence of the emissivity with radius. The continuum is assumed to be a power-law characterized by two parameters – photon index Γ and a normalization factor. Thus the total number of free parameters used for the fitting is six.

3.2. Comptonization model

In this model the intrinsic spectrum is assumed to be a power-law with photon index Γ and a narrow Gaussian line with $\sigma = 0.05$ keV and centroid energy $E = 6.4$ keV. The source is assumed to be surrounded by a highly ionized cloud with optical depth $\tau = n\sigma_T R$ at a temperature kT. The output spectrum is calculated using the Kompane'ets equation. It is important to note that for self consistency both the intrinsic power-law and Iron line are Comptonized by the surrounding cloud. Thus the Comptonization model has seven parameters – τ, kT, the intrinsic photon index Γ, the line energy (fixed at 6.4 keV), the intrinsic width of the line (fixed at 0.05 keV), the line intensity and a normalization factor. Thus the total number of free parameters used for the fitting is five.

from the medium intensity state. Much of the spectral change can be attributed to the slight change in the power-law slope. The line shape during the low intensity level is different from that of the medium intensity data (Table 1). The line is broader as indicated by the increase in the the emissivity index ($\xi = 3.3^{+0.3}_{-0.6}$). The data is again well fit by the model with χ^2/ (dof)= 967/(1424).

The Comptonization model also fits the medium energy data well with χ^2/ (dof)= 1396/(1423) although with a higher χ^2 than the disk line model (Table 2). The temperature of the Comptonizing cloud is found to be $kT = 0.54^{+0.20}_{-0.19}$ keV. This is hotter than the temperature estimated by best fit line profile for the disk line model which was $kT < 0.2$ keV (Fabian et al. 1995, Misra & Kembhavi 1998). The reason for this discrepancy is that fitting the data to this model reveals a blue wing (Figure 2). The low and high intensity data sets are fit after fixing $kT = 0.54$. The high intensity data is well fit by this model χ^2/ (dof)= 1225/(1424) (see Table 2). The fit is similar to the disk line model and again there seems to be evidence for an additional narrow component. Compared to the medium intensity fit the optical depth and line strength have increased while the power-law index (Γ) remain unchanged within the limits of error. Thus in terms of the Comptonization model, the photon index variation in the disk line model fit can be attributed to change in degree of Comptonization of the intrinsic continuum. However, the low statistics of the data set and the presence of an additional narrow line does not allow for any concrete statements to be made. The low intensity data is well fit with a larger optical depth $\tau = 6.7$ with χ^2/ (dof)= 969/(1424). The larger optical depth leads to a broader line for this set.

Since the data is from a narrow band (3 - 10 keV) both the spectral slopes of the broken power-law model cannot be constrained. The medium intensity data is fit to the broken power-law model with the high energy photon index fixed at 2.0. This gives an

3.3. Broken power-law model

The broken power-law is an empirical model used to test the hypothesis that the Iron line in this source is narrow and the artificial broadening observed is due to complexities in the underlying continuum. The Iron line is assumed to be a Gaussian with width $\sigma = 0.2$ keV and centroid at 6.4 keV. The continuum is fit by a broken power-law characterized by a high energy photon index Γ_1, a low energy photon index Γ_2, a break energy E_B and normalization. Thus the total number of free parameters used for the fitting is five.

4. Results

The medium intensity data was fit to the disk line model of Laor (1991) for later comparison with the Comptonization model. The fit parameters are shown in Table 1 and the unfolded data is plotted in Figure 1. As mentioned by Iwasawa et al. (1996) this model fits the data well with $\chi^2/$ (dof)= 1377/(1421) (Table 1, first row). The inner radius $r_i(= 2.9r_s)$ is constrained to be less than $3.7r_s$. However, since the line is broader during the low intensity phase, the inner radius is probably close to 1.235 corresponding to a maximally rotating black hole. Fixing $r_i = 1.235r_s$ and refiting the data gave a $\Delta\chi^2 = 1.0$ (Table 1, second row).

The low and high intensity data sets are fit after fixing $r_i = 1.235$, $r_o = 16.4$ and inclination angle $\phi = 32^o$. These parameters are not expected to change during the observation period and freezing them constrains the rest of the parameters. Moreover the the number of free parameters become equal to those of the Comptonization model (see below) which enables a direct comparison. The high intensity data set is formally well fit by the model with $\chi^2/$ (dof)= 1235/(1424) (see Table 1). There seems to be evidence for an additional narrow component. The emissivity index ($\xi = 2.1^{+0.5}_{-0.7}$) does not vary significantly

Table 1: Spectral parameters for the disk line model of Laor (1991) for the intensity selected data sets. The parameters are the power-law photon index (Γ), the emissivity index (ξ), the inner radius (r_i) in r_s, the outer radius (r_o) in r_s, the line Intensity (I_{line} in units of 10^{-4} photons/sec/cm^2 and the inclination angle ϕ in degrees. The line energy is fixed at 6.4 keV.

Data set	Γ	ξ	r_i	r_o	I_{line}	ϕ	χ^2/ (dof)
Medium	$2.05^{+.04}_{-.03}$	$1.9^{+0.7}_{-0.6}$	$2.9^{+0.8}_{-1.7}$	$16.4^{+1.6}_{-1.0}$	$2.1^{+0.3}_{-0.3}$	$32^{+1.5}_{-2.0}$	1377/(1421)
Medium	$2.05^{+.034}_{-.03}$	$1.8^{+0.4}_{-0.2}$	1.235	16.4	$2.25^{+0.25}_{-0.3}$	32	1378/(1424)
High	$2.20^{+.06}_{-.06}$	$2.0^{+0.7}_{-0.7}$	1.235	16.4	$2.89^{+0.82}_{-0.66}$	32	1235/(1424)
Low	$2.03^{+.19}_{-.18}$	$3.26^{+0.31}_{-0.54}$	1.235	16.4	$2.96^{+0.98}_{-0.91}$	32	967/(1424)

Table 2: Spectral parameters for the Comptonization model for the intensity selected data sets. The parameters are the power-law photon index (Γ), the optical depth (τ), the temperature of the cloud (kT) in keV and the line Intensity (I_{line}) in units of 10^{-4} photons/sec/cm^2. The line energy is fixed at 6.4 keV and the intrinsic line width is assumed to be $\sigma = 0.05$ keV.

Data set	Γ	τ	kT	I_{line}	χ^2/ (dof)
Medium	$1.93^{+.05}_{-.015}$	$4.16^{+0.33}_{-0.49}$	$0.54^{+0.2}_{-0.19}$	$2.22^{+0.55}_{-0.36}$	1396/(1423)
High	$1.96^{+.12}_{-.05}$	$5.32^{+0.62}_{-0.94}$	0.54	$3.71^{+1.07}_{-1.03}$	1225/(1424)
Low	$1.76^{+.18}_{-.44}$	$6.69^{+2.37}_{-1.20}$	0.54	$3.81^{+2.84}_{-1.69}$	969/(1424)

unacceptable fit with $\chi^2/$ (dof)= 1506/(1424). Acceptable fit is obtained if the high energy photon index is set to 2.5 with $\chi^2/$ (dof)= 1422/(1424). The high and low intensity data sets can also be fit by this model provided the high energy photon index is 2.5 (Table 3).

5. Discussion

The fit to the disk line model to the medium and low intensity data set is marginally better than for the Comptonization model. The reduced χ^2 for both the models are less than unity. The reason for this degeneracy is that the spectral shape of the best fit disk line model does not have a clear double peaked feature (Figure 1). Instead the red wing of the line gradually extends to ≈ 5 keV and such a feature can also be due Compton down-scattering of photons. Thus, the narrow band (3 - 10 keV) data used here cannot differentiate between these two models.

Although the high intensity data set is formally well fit by the models, there is evidence for an additional narrow Iron line (Iwasawa et al. 1996) in the residual plots. This could be due to a real additional narrow Iron line (Sulentic, Marziani & Calvani 1998). An alternate explanation could be that the Iron line shape is variable in a time scale shorter than the observation time ($\approx 10^5$ secs). In such a scenario the observed shape of the Iron line would be the time-averaged profile and would not fit the time-independent modeling.

Since there are no strong absorption lines in this source the size of the Comptonizing cloud has to be smaller than $R < 10^{14}$ cms (Fabian et al. 1995). For a $10^6 M_\odot$ black hole this corresponds to about $\approx 300 r_s$. The intrinsic Iron line produced in this case will not be significantly broadened by gravitational red-shift or Doppler effects. However if the black hole mass is larger, these effects would be important and the observed profile would be complex combination of Comptonization and gravitational effects. In this work for simplicity we have assumed that the intrinsic line is narrow ($\sigma = 0.05$ keV). The temperature of this cloud can be determined by equating the heating and cooling of the gas by Compton scattering. As described by Misra & Kembhavi (1998) the temperature of the gas depends upon the assumed UV flux of the intrinsic source. In Figure 3, the dashed line shows the assumed intrinsic spectrum for the source. The solid line is the output spectrum after the radiation passes through the cloud with optical depth $\tau = 4.0$ (the best fit value for the medium intensity data). The temperature of the cloud was calculated by balancing the input radiative power to the output power. The UV flux has been assumed here such that this temperature is equal to the best fit value $kT \approx 0.55$ keV. The UV luminosity is lower than that estimated by Misra & Kembhavi (1998) since the best fit value of the temperature is 0.5 keV and not 0.2 keV as has been assumed earlier. The shape of the UV bump has been assumed here to have a black-body like shape. However, the equilibrium temperature is not sensitive to the spectral shape but rather to the total luminosity in the UV band compared to the X-ray band. The UV flux in MCG-6-30-15 is highly reddened and hence a UV bump is not directly observed for this source (Reynolds et al. 1997). Using the minimum value for the extinction, a lower limit of the intrinsic flux (F_{min}) has been calculated by Reynolds et al (1997) and is plotted in Figure 3 for comparison. The UV flux required by this model is about a factor ten larger than this minimum value. The reprocessed IR emission from covering dust in this source also indicate that the UV flux is much larger than F_{min} (Reynolds et al 1997).

The temperature of the gas will react to the changing intrinsic spectrum in a time scale set by the time for the photons to diffuse out of the system,

$$t_c \approx (\frac{R}{c})\tau^2 = 8 \times 10^4 \mathrm{secs}(\frac{R}{10^{14} cm})(\frac{\tau}{5})^2 \quad (1)$$

The dynamical time scale is

$$t_d \approx (\frac{R}{v}) \approx= 6 \times 10^4 \mathrm{secs}(\frac{R}{10^{14} cm})^{1/2}(\frac{M}{10^6 M_\odot})^2 \quad (2)$$

where $v \approx (2GM/R)^{1/2}$ is the average bulk velocity of the plasma. Since this two time-scales are comparable to the observation time scale , the temperature and the optical depth can vary during the observations. The data is compatible with no change in temperature during the observation period with the change in the line profile being attributed to changes in the optical depth of the cloud (Table 2).

The continuum spectrum for energies ($E > 20$ keV) is greatly affected by the presence of a Comptonizing medium. For $E > 100$ keV the decrease in flux is nearly half of what is expected from a simple power-law model (Figure 3). The averaged Seyfert 1 spectrum from OSSE has been presented by Gondek et al. (1996). They find that at $E = 100$ keV, there is no significant decrease in the flux from the extrapolated power-law value. However, the statistics is not good enough to rule out a 50% decrease in flux. Moreover the spectrum is an average one and thus it may not represent MCG-6-30-15 actual spectrum. Significant differences in the continuum spectrum is also expected for $20 < E < 100$ keV. The analysis in this energy range is complicated by the presence of the reflection component which is significant only for $15 < E < 60$ keV. Nandra & Pounds (1994) analyzed the Ginga data for this source in $2 < E < 18$ keV range and find that a reflection component corresponding to a solid angle $\Omega_r \approx 2.0\pi$ is required to explain the data. This indicates that there is an excess flux at $E > 15$ keV which is in apparent contradiction to the Comptonization model. This excess can be explained within the framework of the Comptonization model if the intrinsic reflection component has a higher value of $\Omega_r \approx 2.4\pi$ (Misra & Kembhavi 1998). For $E > 20$ keV, the difference between the Comptonized power-law and power-law model is larger and can only be removed by invoking an extremely large unphysical solid angle for the reflected component $\Omega_r > 5\pi$. Thus broad-band ($3 < E < 50$ keV) coverage of this source will definitely rule out or confirm the Comptonization model. An additional complication arises because the source (and hence the Comptonizing cloud) is known to be variable. Hence simultaneous observation in this range will be required.

Another explanation for these observations could be that the intrinsic line is narrow but the underlying continuum is complex i.e. not just a simple power-law. To test this hypothesis we have fit the data to a narrow line and a broken power-law. We find that the high energy spectral index has to be ≈ 2.5 for this model to fit the data. The Ginga data seems to contradict this result since the spectral index obtained was ≈ 2.0. If simultaneous broad band data ($3 < E < 50$ keV) can confirm this result that the spectral index is ≈ 2.0 and not ≈ 2.5 this empirical model can be ruled out. It is also not clear which physical process will give a break energy $E_b \approx 5$ keV (Table 3).

6. Summary

The disk line model and the Comptonization model can fit the Iron profile of this source for the low and medium intensity data sets. The width and skewness of the Iron line profile can be reproduced if the source is surrounded by a cloud with optical thickness $\tau \approx 4$ and temperature $kT \approx 0.6$ keV. This temperature is higher than earlier estimates based on fits using the disk line model. The cloud will have this temperature provided there is a UV bump in the source which is not visible due to extinction.

The Iron line profile could also be narrow if the underlying continuum is complex. Modeling the continuum as a broken power-law allows for a reasonable fit only if the high energy photon spectral is ≈ 2.5 which may be in conflict with the earlier Ginga observations.

Simultaneous broad band ($3 - 50$ keV) observations of this source will be able to rule out (or confirm) the Comptonization model. Such an exercise will strongly constrain any theoretical accretion disk models invoked to explain the AGN phenomena.

The authors would like to thank S. Raychoudhary and A. Kembhavi for useful discussions.

Table 3: Spectral parameters for the Broken power-law model for the intensity selected data sets. The parameters are the high energy power-law photon index (Γ_1), the low energy power-law photon index (Γ_2), the break energy (E_b) in keV and the line Intensity (I_{line} in units of 10^{-4} photons/sec/cm^2. The line energy is fixed at 6.4 keV and the intrinsic line width is assumed to be $\sigma = 0.2$ keV.

Data set	Γ_1	Γ_2	E_b	I_{line}	χ^2/ (dof)
Medium	2.5	$1.77^{+0.03}_{-0.03}$	$5.81^{+0.13}_{-0.15}$	$0.48^{+0.09}_{-0.08}$	1422/(1424)
High	2.5	$1.91^{+0.05}_{-0.06}$	$5.28^{+0.27}_{-0.12}$	$0.96^{+0.16}_{-0.23}$	1208/(1424)
Low	2.5	$1.45^{+0.10}_{-0.15}$	$5.30^{+0.29}_{-0.26}$	$0.27^{+0.19}_{-0.17}$	972/(1424)

REFERENCES

Czerny B., Zbyszewska M. & Raine, D.J. 1991, in Treves A., ed., Iron line Diagnostics in X-ray Sources, Springer-Verlag, Berlin, p 226.

Fabian, A.C., Rees, M.J., Stella, L. & White, N.E. 1989, MNRAS, **238**, 729.

Fabian, A.C. et al. 1995, MNRAS, **277**, L11.

Gondek, D. et al. 1996, MNRAS, **282**, 646.

Guilbert, P. W. & Rees, M.J., 1988, MNRAS, **292**, 664.

Iwasawa, K. 1996, MNRAS**282**, 1038.

Kuncic, E.G., Blackman, E. G. & Rees, M.J., 1996, MNRAS, **283**, 1322.

Laor, A., 1991, ApJ, **376**, 90.

McKernan, B. & Yaqoob, T., 1998, ApJ, in press.

Misra, R. & Kembhavi, A.K., 1998, ApJ, **499**, in press .

Nandra, K. & Pounds, K.A. 1994, MNRAS, **268**, 405.

Nandra, K., George, I.M., Mushotzsky, R.F., Turner, T.J. & Yaqoob, T. 1997, ApJ, **477**, 602.

Reynolds, C. S. & Begelman M. C. 1997, ApJ, **488**, 109.

Reynolds et al., 1997, MNRAS, **291**, 403.

Sulentic, J. et al., 1998, ApJ, in press.

Sulentic, J., Marziani, P. & Calvani, M., 1998, ApJ, **497**, L65

Tanaka, Y., Inoue, H. & Holt, S.S., 1994, PASJ, **46**, L137

Tanaka, Y. et al., 1995, Nature, **375**, 659.

This manuscript was prepared with the AAS LaTeX macros v4.0.

Fig. 1.— The unfolded spectra and best fit disk line model of Laor (1991). The medium intensity data from the four chips are shown separately. The dotted line is the power-law while the solid line is the sum of the power-law and Iron line profile. The parameters of the fit are given in Table 1.

Fig. 2.— The unfolded spectra and best fit Comptonization model. The medium intensity data from the four chips are shown separately. The dotted line is the Comptonized power-law while the solid line is the sum of the power-law and Iron line profile. The parameters of the fit are given in Table 2.

Fig. 3.— The Comptonized multi-wavelength spectrum for MCG-6-30-15. The dotted line is the assumed intrinsic spectrum of the source while the solid line is the Comptonized one. The intrinsic component consists of a UV bump, a X-ray power-law and a reflection component. The flux of the UV bump is chosen such that the equilibrium temperature of the surrounding cloud is $kT = 0.55$ keV. Also shown is the UV lower limit for this source (Reynolds et al. 1997). Maximum deviation occurs for $E > 50$ keV.

Figure 1

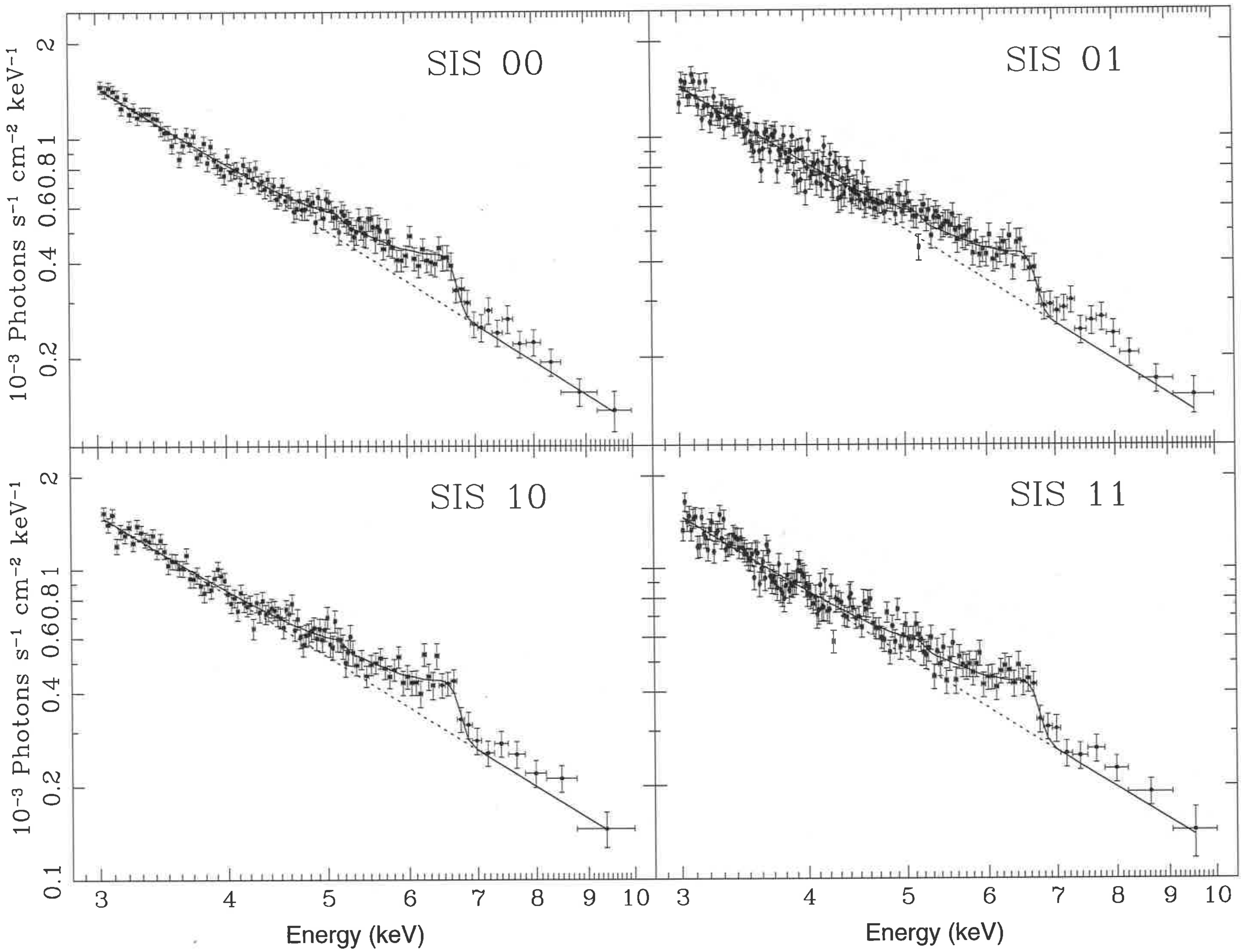
SIS 00
SIS 01
SIS 10
SIS 11
10^-3 Photons s^-1 cm^-2 keV^-1
0.1
0.2
0.4
0.6
0.8
1
2
3
4
5
6
7
8
9
10
Energy (keV)